Indian Journal of Pure & Applied Physics
Vol. 56, July 2018, pp. 551-560

Numerical investigation on viscous dissipating and chemically reacting fluid over an impulsively started vertical cylinder

P Loganathan[a]* & M Dhivya[b]

[a]Department of Mathematics, College of Engineering, Guindy, Anna University, Chennai 600 025, India

[b]Department of Mathematics, College of Engineering, Guindy, Anna University, Chennai 600 025, India

Received 11 October 2017; accepted 27 December 2017

The present analysis deals with the numerical investigation of an unsteady laminar free convective flow of a viscous, incompressible, dissipative, electrically conducting, optically thin and chemically reacting fluid past a moving semi-infinite vertical cylinder embedded in a porous medium. The problem has been governed by a system of coupled nonlinear boundary layer equations with appropriate initial and boundary conditions. These governing equations have been reduced to a non-dimensional form and have been solved numerically using Crank-Nicholson implicit finite difference method, which is unconditionally stable and convergent. The influence of physical parameters such as Prandtl number, Schmidt number, Eckert number, Grashof number for heat transfer, Grashof number for mass transfer, permeability parameter, magnetic parameter, radiation parameter and chemical reaction parameter on velocity profiles, temperature profiles, concentration profiles, local skin-friction coefficient, mean skin-friction coefficient, local Nusselt number, mean Nusselt number, local Sherwood number and mean Sherwood number have been shown graphically. An increase in the value of Eckert number increases the velocity and temperature. Also, the rate of heat transfer and mass transfer gets enhanced for decreasing values of the Eckert number.

Keywords: Moving vertical cylinder, Finite difference scheme, Porous medium, Viscous dissipation, Thermal radiation

1 Introduction

Studies on convective flow over a moving vertical cylinder have received a notable interest among researchers because of its applications in science and engineering. It has several applications in the devices of heat exchangers, in manufacturing processes for the design of propulsion devices of aircraft and also in nuclear reactors. Similarly, flow past an impulsively started vertical cylinder embedded in a porous medium has applications in solar energy porous water collector systems and nuclear waste disposal. The porous medium is specified by its permeability which measures the flow conductivity in a porous medium. Natural convective flow through a vertical cylinder embedded in a porous medium was analyzed by Minkowcycz and Chen[1] and also by Yucel[2].

Viscous dissipation (VD) effect plays a major role in the case, where the induced kinetic energy is predominant compared to the amount of heat transferred. If the viscosity of the fluid is high and the thermal conductivity is low then the VD effects are highly significant. It can also be incorporated, when the gravitational field is strong.

*Corresponding author (E-mail: logu@annauniv.edu)

VD occurs in natural convection, if the devices are subjected to large decelerations. In addition to this, during natural convection viscous generation of heat will affect the flow when the flow fields are of extreme size. Gebhart[3,4] made an excellent analysis on free convective flow, when VD takes place. Basu *et al*.[5] also investigated the same kind of problem for a tube.

Heat transfer takes place due to natural convection in the presence of porous medium under the influence of VD was studied by Nayakama and Pop[6]. Later on, the influence of VD and radiation on a vertical annular cylinder embedded in a porous medium due to natural convection was analyzed by Badruddin *et al*.[7] using Finite element method. The study of first order chemical reaction, thermal radiation and MHD effect on an unsteady natural convective flow over a moving vertical plate was given by Muthucumaraswamy *et al*[8]. Poonia and Chaudhary[9] examined about mixed convection in the presence of VD effect for an electrically conducting fluid over a cooling plate. It was concluded that an increase in the Eckert number corresponds to viscous dissipation effects increases the temperature of the cooling plate. The same type of problem for heating

plate with homogeneous chemical reaction was discussed by Rao and Shivaiah[10].

Combined heat and mass transfer effects for an electrically conducting and chemically reacting fluid on a moving porous plate with radiation and VD was investigated by Babu *et al.*[11]. Singh[12] studied about natural convective flow with chemical reaction and Magneto hydrodynamics (MHD) on an inclined plate for steady state. An explicit finite difference scheme was applied to study the effects of thermal radiation, MHD and VD of nanofluid along a stretching sheet due to free convection by Khan *et al.*[13]. It was mentioned that dissipation is the process of converting mechanical energy of downward-flowing water into thermal and acoustical energy.

Ibrahim and Reddy[14] analyzed the same kind of problem for the case of internal heat generation. In this problem, the solutions are obtained using shooting technique. The study on an unsteady MHD, radiative and chemically reacting fluid past a moving vertical plate with temperature was made by Reddy[15]. The same kind of problem for a nanofluid along the stretching sheet was examined by Haile and Shankar[16]. Mixed convective flow over a vertical plate immersed in a porous medium with the effects of VD and thermal radiation was studied by Narayana *et al.*[17]. Steady state analysis for mixed convective flow of a second grade fluid over a stretching sheet under the influence of chemical reaction and VD was examined by Das[18].

Heat and mass transfer effects of an unsteady MHD, radiative and chemically reacting fluid with variable surface temperature and concentration was analyzed using an implicit finite difference scheme by Ahmed *et al.*[19]. Later, Raju *et al.*[20] gave the analytical solution for free convective, dissipative, chemically reactive, radiative and electrically conducting fluid past a porous vertical surface in the presence of constant suction. It was inspected that the influence of magnetic field and radiation decreases the velocity and temperature.

Reddy *et al.*[21] studied the effects of VD, chemical reaction and radiation on MHD free convective flow over an moving infinite vertical plate. It was mentioned that this type of problem has applications in industrial and geothermal processes. Galerkin method was employed to study the same kind of problem with variable surface temperature and concentration for a stationary vertical plate by Balla and Naikoti[22].

Sheri and Raju[23] investigated the effects of VD on MHD free convective flow over an infinite vertical plate in the presence of porous medium and it was mentioned that it has applications in MHD pumps and MHD bearings. Perturbation technique was employed to study the effects of chemical reaction, thermal radiation and soret number on Magnetohydramic heat and mass transfer of a casson fluid in the presence of magnetic field and VD by Pal and Biswas[24].

Recently Sreedevi *et al.*[25] investigated the heat and mass transfer effects of natural convection past a permeable stretching sheet in the presence of VD, chemical reaction, MHD, thermal radiation, Soret and Dufour effects and it was concluded that increasing the values of thermal radiation, VD and chemical reaction results in the increase of velocity, temperature and rate of heat and mass transfer. Reddy *et al.*[26] examined the influence of VD and MHD effects on an unsteady free convective flow of a casson fluid on a stretching sheet using finite element method. The study of natural convection flow of a nanofluid due to stretching cylinder in a porous medium along with VD and slip boundary conditions was analyzed using shooting technique by Pandey and Kumar[27].

This article deals with the heat and mass transfer effects on transient free convective flow of a laminar, viscous, incompressible, chemically reacting fluid about a moving permeable vertical cylinder in the presence of transverse magnetic field. The effect of viscous dissipation is also taken into account. The governing boundary layer equations are solved numerically, using Crank-Nicholson implicit scheme and the behaviour of velocity, temperature and concentration are depicted graphically.

2 Mathematical Analysis

Consider the transient free convective flow of a Newtonian, viscous, incompressible, chemically reacting and electrically conducting fluid past a semi-infinite moving vertical cylinder embedded in a porous medium. The radius of the cylinder is taken as r_0. The *x*-axis is measured vertically upward along the axis of the cylinder and the radial co-ordinate *r* is measured perpendicular to the axis of the cylinder. In this problem T'_∞, C'_∞, T'_w and C'_w are taken as free stream temperature, free stream concentration, wall temperature and wall concentration, respectively. Initially, both cylinder and the fluid are kept stationary at the same temperature T'_∞ and also at the

same concentration level $C_\infty^{'}$. The physical model of the problem is depicted in Fig. 1.

At time $t^{'} > 0$, the cylinder starts moving in the vertical direction with velocity u_0. At that time the temperature and concentration level on the surface of the cylinder are taken to be $T_w^{'} > T_\infty^{'}$ and $C_w^{'} > C_\infty^{'}$ respectively. In the energy equation, viscous dissipation effect is included and it is assumed that the radiative heat flux along the axial direction is negligible compared to that in the radial direction. A uniform magnetic field B_0 is assumed to be applied in a direction perpendicular to the surface of the cylinder. The first order homogeneous, irreversible chemical reaction takes place in the axial direction. The gravitational acceleration g is acting downward. Under these assumptions along with the Boussinesq approximation, the equations of continuity, momentum, thermal energy and mass diffusion for the laminar boundary layer flow can be written as:

$$\frac{\partial (ru)}{\partial x} + \frac{\partial (rv)}{\partial r} = 0 \qquad \ldots (1)$$

$$\frac{\partial u}{\partial t^{'}} + u\frac{\partial u}{\partial x} + v\frac{\partial v}{\partial r} = g\beta (T^{'} - T_\infty^{'}) + g\beta^{*}(C^{'} - C_\infty^{'}) + \frac{\upsilon}{r}\frac{\partial}{\partial r}\left(r\frac{\partial u}{\partial r}\right) - \frac{\upsilon}{\lambda^{*}}u - \frac{\sigma B_0^2 u}{\rho} \qquad \ldots (2)$$

$$\frac{\partial T^{'}}{\partial t^{'}} + u\frac{\partial T^{'}}{\partial x} + v\frac{\partial T^{'}}{\partial r} = \frac{\alpha}{r}\frac{\partial}{\partial r}\left(r\frac{\partial T^{'}}{\partial r}\right) + \frac{\mu}{\rho C_p}\left(\frac{\partial u}{\partial r}\right)^2 + \frac{1}{\rho C_p}\frac{1}{r}\frac{\partial}{\partial r}(r\, q_r) \qquad \ldots (3)$$

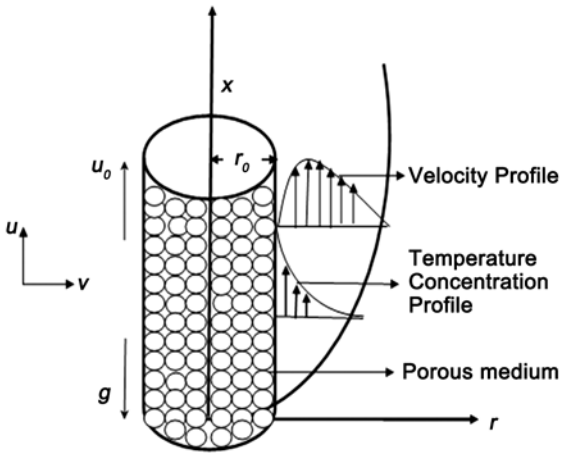

Fig. 1 — Physical model of the problem.

$$\frac{\partial C^{'}}{\partial t^{'}} + u\frac{\partial C^{'}}{\partial x} + v\frac{\partial C^{'}}{\partial r} = \frac{D}{r}\frac{\partial}{\partial r}\left(r\frac{\partial C^{'}}{\partial r}\right) - K_r^{'}(C^{'} - C_\infty^{'}) \qquad \ldots (4)$$

with initial and boundary conditions:

$$\begin{aligned} &t^{'} \le 0 \quad u = 0, v = 0, T^{'} = T_\infty^{'}, C^{'} = C_\infty^{'} \text{ for all } x \text{ and } r \\ &t^{'} > 0 \quad u = u_0, v = 0, T^{'} = T_w^{'}, C^{'} = C_w^{'} \text{ at } r = r_0 \\ &u = 0, T^{'} = T_\infty^{'}, C^{'} = C_\infty^{'} \text{ at } x = 0 \text{ and } r \ge r_0 \\ &u \to 0, T^{'} \to T_\infty^{'}, C^{'} \to C_\infty^{'} \text{ as } r \to \infty \end{aligned} \qquad \ldots (5)$$

where u and v are velocity components in x and r directions, respectively, $t^{'}$ is the time, $T^{'}$ is the dimensional temperature, $C^{'}$ is the dimensional concentration, β is the volumetric coefficient of thermal expansion, β^{*} is the volumetric coefficient of expansion with concentration, μ is the dynamic viscosity, υ is the kinematic viscosity, λ^{*} is the dimensionless permeability, ρ is the density, σ is the electrical conductivity of the fluid, α is the thermal diffusion coefficient, C_p is the specific heat at constant pressure, D is the mass diffusivity, q_r is the radiative heat flux and $K_r^{'}$ is the chemical reaction parameter.

According to Brewster[28], using Rosseland approximation, the radiative heat flux q_r can be considered as:

$$q_r = -\frac{4\sigma_s}{3\kappa^{*}}\frac{\partial T^{'4}}{\partial r} \qquad \ldots (6)$$

where σ_s is the Stefan-Boltzmann constant and κ^{*} is the mean absorption coefficient. It is observed that the present analysis is restricted to optically thin fluids, due to Rosseland approximation.

If the temperature differences within the flow are sufficiently small such that $T^{'4}$ may be expressed as a linear function of the temperature, then $T^{'4}$ can be expressed using Taylor series about $T_\infty^{'}$ and neglecting higher order terms, it is given by:

$$T^{'4} \cong 4T_\infty^{'3}T^{'} - 3T_\infty^{'4} \qquad \ldots (7)$$

As a result of Eqs (6) and (7), Eq. (3) reduces to:

$$\frac{\partial T^{'}}{\partial t^{'}} + u\frac{\partial T^{'}}{\partial x} + v\frac{\partial T^{'}}{\partial r} = \frac{\alpha}{r}\frac{\partial}{\partial r}\left(r\frac{\partial T^{'}}{\partial r}\right) + \frac{\mu}{\rho C_p}\left(\frac{\partial u}{\partial r}\right)^2 + \frac{16\sigma T_\infty^{'3}}{3\rho C_p \kappa^{*}}\frac{1}{r}\frac{\partial}{\partial r}\left(r\frac{\partial T^{'}}{\partial r}\right) \qquad \ldots (8)$$

Introducing the following non-dimensional quantities:

$$X=\frac{x\upsilon}{r_0^2 u_0},\quad R=\frac{r}{r_0},\quad U=\frac{u}{u_0},\quad V=\frac{vr_0}{\upsilon},$$

$$t=\frac{t'\upsilon}{r_0^2},\quad T=\frac{T'-T'_\infty}{T'_w-T'_\infty},\quad C=\frac{C'-C'_\infty}{C'_w-C'_\infty}$$

$$Gr=\frac{g\beta r_0^2(T'_w-T'_\infty)}{\upsilon u_0},\quad Gc=\frac{g\beta^* r_0^2(C'_w-C'_\infty)}{\upsilon u_0},$$

$$Pr=\frac{\upsilon}{\alpha},\quad \lambda=\frac{\lambda^*}{r_0^2},\quad M=\frac{\sigma B_0^2 r_0^2}{\rho\upsilon},$$

$$Ec=\frac{u_0^2}{C_p(T'_w-T'_\infty)},\quad N=\frac{\kappa^* k}{4\sigma T'^3_\infty},$$

$$Sc=\frac{\upsilon}{D},\quad K=\frac{K'_r r_0^2}{\upsilon} \qquad \text{... (9)}$$

Using non-dimensional quantities in Eq. (9), Eqs (1), (2), (8) and Eq. (4) are reduced to the following form:

$$\frac{\partial(RU)}{\partial X}+\frac{\partial(RV)}{\partial R}=0 \qquad \text{... (10)}$$

$$\frac{\partial U}{\partial t}+U\frac{\partial U}{\partial X}+V\frac{\partial U}{\partial R}=\frac{1}{R}\frac{\partial}{\partial R}\left(R\frac{\partial U}{\partial R}\right)+Gr\,T+Gc\,C-M\,U-\frac{U}{\lambda} \qquad \text{... (11)}$$

$$\frac{\partial T}{\partial t}+U\frac{\partial T}{\partial X}+V\frac{\partial T}{\partial R}=\left(1+\frac{4}{3}N\right)\frac{1}{Pr}\frac{1}{R}\frac{\partial}{\partial R}\left(R\frac{\partial T}{\partial R}\right)+Ec\left(\frac{\partial U}{\partial R}\right)^2 \qquad \text{... (12)}$$

$$\frac{\partial C}{\partial t}+U\frac{\partial C}{\partial X}+V\frac{\partial C}{\partial R}=\frac{1}{Sc}\frac{1}{R}\frac{\partial}{\partial R}\left(R\frac{\partial C}{\partial R}\right)-K\,C \qquad \text{... (13)}$$

The corresponding initial and boundary conditions in non-dimensional quantities are given by:

$$t\le 0:\ U=0,\ V=0,\ T=0,C=0 \text{ for all } X \text{ and } R$$
$$t>0:\ U=1,\ V=0,\ T=1,\ C=1 \text{ at } R=1$$
$$U=0,\ T=0,\ C=0 \text{ at } X=0 \text{ and } R\ge 1$$
$$U\to 0,\ T\to 0, C\to 0 \text{ as } R\to\infty \qquad \text{... (14)}$$

where U and V are velocity components in dimensionless axial coordinate X and radial coordinate R respectively, t is the dimensionless time, T is the temperature, C is the concentration, Gr, Gc, M, λ, N, Pr, Ec, Sc, K are the Grashof number for heat transfer, Grashof number for mass transfer, Magnetic parameter, permeability parameter of the porous medium, radiation parameter, Prandtl number, Eckert number, Schmidt number and dimensionless chemical reaction parameter, respectively.

3 Numerical Technique

Equation (10-13) consists of a system of coupled, non-linear, partial differential equations. These equations along with the initial and boundary conditions are given in Eq. (14) have been solved using implicit finite difference scheme of Crank Nicholson type. The finite difference scheme corresponding to Eqs (10-13) are as follows:

$$\frac{U_{i,j-1}^{m+1}-U_{i-1,j-1}^{m+1}+U_{i,j}^{m+1}-U_{i-1,j}^{m+1}}{4\Delta X}+\frac{U_{i,j-1}^{m}-U_{i-1,j-1}^{m}+U_{i,j}^{m}-U_{i-1,j}^{m}}{4\Delta X}+\frac{V_{i,j}^{m+1}-V_{i,j-1}^{m+1}+V_{i,j}^{m}-V_{i,j-1}^{m}}{2\Delta R}+\frac{V_{i,j}^{m+1}}{[1+(j-1)\Delta R]}=0 \qquad \text{... (15)}$$

$$\frac{U_{i,j}^{m+1}-U_{i,j}^{m}}{\Delta t}+\frac{U_{i,j}^{m}}{2(\Delta X)}\left(U_{i,j}^{m+1}-U_{i-1,j}^{m+1}+U_{i,j}^{m}-U_{i-1,j}^{m}\right)+\frac{V_{i,j}^{m}}{4(\Delta R)}\left(U_{i,j+1}^{m+1}-U_{i,j-1}^{m+1}+U_{i,j+1}^{m}-U_{i,j-1}^{m}\right)=Gr\,\frac{T_{i,j}^{m+1}+T_{i,j}^{m}}{2}+Gc\,\frac{C_{i,j}^{m+1}+C_{i,j}^{m}}{2}+\frac{\left(U_{i,j-1}^{m+1}-2U_{i,j}^{m+1}+U_{i,j+1}^{m+1}\right)}{2(\Delta R)^2}+\frac{\left(U_{i,j-1}^{m}-2U_{i,j}^{m}+U_{i,j+1}^{m}\right)}{2(\Delta R)^2}+\frac{\left(U_{i,j+1}^{m+1}-U_{i,j-1}^{m+1}+U_{i,j+1}^{m}-U_{i,j-1}^{m}\right)}{4(\Delta R)[1+(j-1)\Delta R]}-M\left(\frac{U_{i,j}^{m+1}+U_{i,j}^{m}}{2}\right)-\frac{U_{i,j}^{m+1}+U_{i,j}^{m}}{2\lambda} \qquad \text{... (16)}$$

$$\frac{T_{i,j}^{m+1}-T_{i,j}^{m}}{\Delta t}+\frac{U_{i,j}^{m}}{2(\Delta X)}\left(T_{i,j}^{m+1}-T_{i-1,j}^{m+1}+T_{i,j}^{m}-T_{i-1,j}^{m}\right)+\frac{V_{i,j}^{m}}{4(\Delta R)}\left(T_{i,j+1}^{m+1}-T_{i,j-1}^{m+1}+T_{i,j+1}^{m}-T_{i,j-1}^{m}\right)=\left(1+\frac{4}{3}N\right)\frac{\left(T_{i,j+1}^{m+1}-T_{i,j-1}^{m+1}+T_{i,j+1}^{m}-T_{i,j-1}^{m}\right)}{4Pr[1+(j-1)\Delta R]\Delta R}+\left(1+\frac{4}{3}N\right)\frac{\left(T_{i,j-1}^{m+1}-2T_{i,j}^{m+1}+T_{i,j+1}^{m+1}\right)}{2Pr(\Delta R)^{2}}+\left(1+\frac{4}{3}N\right)\frac{\left(T_{i,j-1}^{m}-2T_{i,j}^{m}+T_{i,j+1}^{m}\right)}{2Pr(\Delta R)^{2}}+Ec\,\frac{\left(U_{i,j+1}^{m+1}-U_{i,j-1}^{m+1}+U_{i,j+1}^{m}-U_{i,j-1}^{m}\right)}{4(\Delta R)}\times\frac{\left(U_{i,j+1}^{m+1}-U_{i,j-1}^{m+1}+U_{i,j+1}^{m}-U_{i,j-1}^{m}\right)}{4(\Delta R)} \quad \ldots (17)$$

$$\frac{C_{i,j}^{m+1}-C_{i,j}^{m}}{\Delta t}+\frac{U_{i,j}^{m}}{2(\Delta X)}\left(C_{i,j}^{m+1}-C_{i-1,j}^{m+1}+C_{i,j}^{m}-C_{i-1,j}^{m}\right)+\frac{V_{i,j}^{m}}{4(\Delta R)}\left(C_{i,j+1}^{m+1}-C_{i,j-1}^{m+1}+C_{i,j+1}^{m}-C_{i,j-1}^{m}\right)=\frac{\left(C_{i,j+1}^{m+1}-C_{i,j-1}^{m+1}+C_{i,j+1}^{m}-C_{i,j-1}^{m}\right)}{4Sc[1+(j-1)\Delta R]\Delta R}+\frac{\left(C_{i,j-1}^{m+1}-2C_{i,j}^{m+1}+C_{i,j+1}^{m+1}\right)}{2Sc(\Delta R)^{2}}+\frac{\left(C_{i,j-1}^{m}-2C_{i,j}^{m}+C_{i,j+1}^{m}\right)}{2Sc(\Delta R)^{2}}-K\left[\frac{C_{i,j}^{m+1}-C_{i,j}^{m}}{2}\right] \quad \ldots (18)$$

In the above Eqs (15-18) the subscript i allocates the grid points along the axial direction $i\Delta X$, the subscript j allocates the grid points along the radial direction $1+(j-1)\Delta R$ and the superscript m allocates the value of time $m\Delta t$. The values of $U_{i,j}^{m}$ and $V_{i,j}^{m}$ occurring in Eqs (15-18) are treated as constants at any one-time step.

Consider the region of integration as a rectangle with sides $X_{\max}(=1.0)$ and $R_{\max}(=15.0)$ where $R_{\max}$ corresponds to $R=\infty$ which lies very well outside the momentum, thermal and concentration boundary layers. The grid independence test has been performed to fix the grid sizes for the problem. After experimenting with a few set of grid sizes, the grid sizes have been fixed at the level $\Delta X=0.02$, $\Delta R=0.20$, with time step $\Delta t=0.01$. In this case, spatial grid sizes are reduced by 50% in one direction and later in both directions and the results are compared then the grid sizes are fixed. If the relative differences between the current and previous iterative values are found to differ only in the fifth decimal place then the iteration process gets terminated. Therefore, the above grid sizes have been considered as appropriate.

The values of velocities, temperature and concentration are calculated by the following process. Initially at time $t=0$, the values of U,V,T and C are known. The values of C,T,U and V at the next time step $t=t+\Delta t$ has to be estimated using the initial conditions specified in the problem. To do so, first and foremost C value is calculated by considering Eq. (18). In Eq. (18) each internal nodal point on a particular level say i-level constitute a tri-diagonal system and it can be solved using Thomas algorithm, which was explained in detail by Carnahan et al.[29]. Applying the same process, the values of T and U are calculated using Eqs (17) and (16), respectively. After obtained the values of C, T and U, the value of V is computed explicitly from Eq. (15). This process gets repeated until it reaches the steady state. The steady state is reached, when the relative difference between successive values differs around five decimal places. In general for every nodal point j on a particular i-level the values of concentration, temperature and velocities are calculated at $(m+1)\Delta t$ time step from $m\Delta t$ time step.

The truncation error in the finite-difference approximation is $O(\Delta t^{2}+\Delta R^{2}+\Delta X)$ and it tends to zero as Δt, ΔX and $\Delta R\to 0$. Hence the scheme is unconditionally stable and convergent.

4 Comparison

In order to examine the accuracy, the solution obtained for temperature and concentration profiles are compared with the results of Chen and Yuh[30] where $Pr = 0.7$, $Sc = 0.2$, $Gr = Gc = 1.0$, $\lambda = 0$, $M = 0$, $Ec = 0$, $N = 0$, $K = 0$ (corresponding to $\xi = 4$) and it is found to be an excellent match as shown in Fig. 2.

5 Results and Discussion

Figure 3 illustrates the influence of Eckert number and Grashof number on the velocity for the case of air $Pr = 0.7$ at $X = 1.0$. It is examined that increasing the value of Gr and Gc increases the velocity. This implies that the velocity curve increases at a slow pace reaches a maximum value and decreases gradually near the wall of the cylinder as Gr increases. The values of Gr and Gc under consideration are large due to natural convection. Time taken to reach steady state decreases with increasing values of Gr and Gc. Increasing the value of Eckert number leads to an increase in the velocity due to the induced kinetic energy. This implies that if viscous dissipation is highly significant then the fluid flows quickly. Also, the time taken to reach steady state decreases with increasing values of Eckert number.

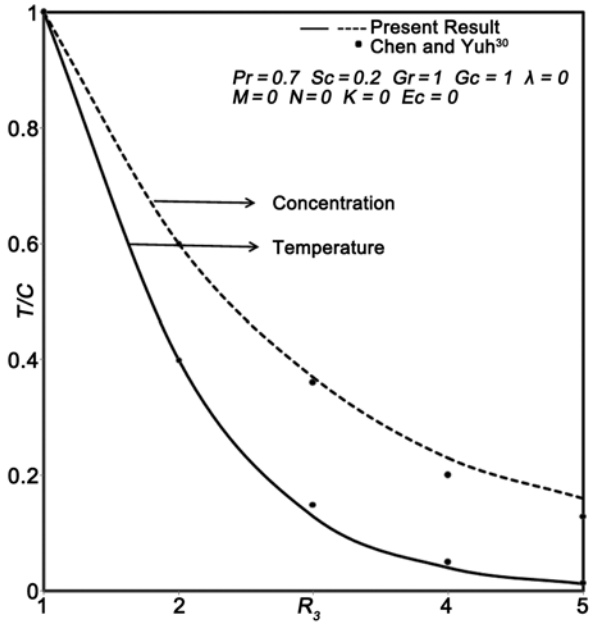

Fig. 2 — Comparison of temperature and concentration profiles.

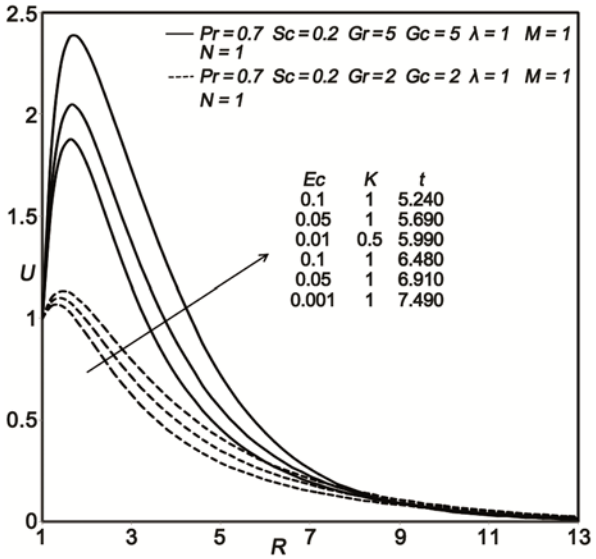

Fig. 3 — Velocity profiles for steady state.

Figure 4 shows the steady state velocity profiles for various values of the permeability parameter λ at $X = 1.0$. It is observed that velocity increases as λ increases. It is also perceived that the time taken to reach steady state increases with increasing values of the permeability parameter λ.

Figure 5 illustrates the influence of magnetic parameter M on the velocity for the case of air $Pr = 0.7$ at $X = 1.0$. It is inspected that increasing the value of M leads to a decrease in velocity. This is due to the application of transverse magnetic field to an electrically conducting fluid which gives rise to a force called Lorentz force. This force makes the fluid to flow in a slow pace and it retards the velocity. Time taken to reach steady state increases with increasing value of the magnetic parameter M.

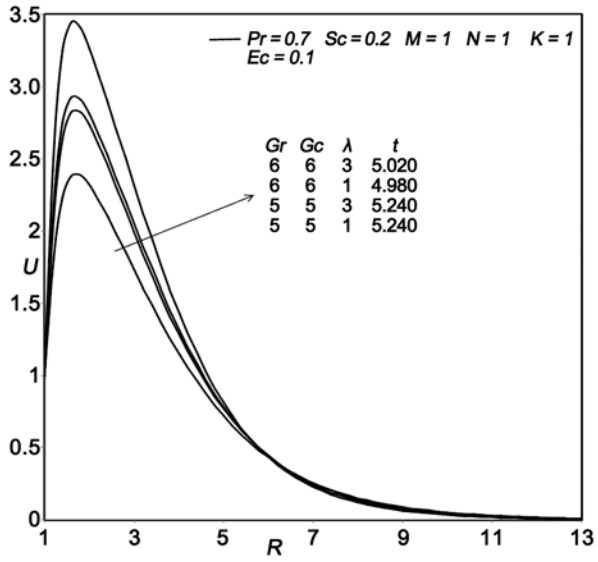

Fig. 4 — Velocity profile for Permeability parameter λ.

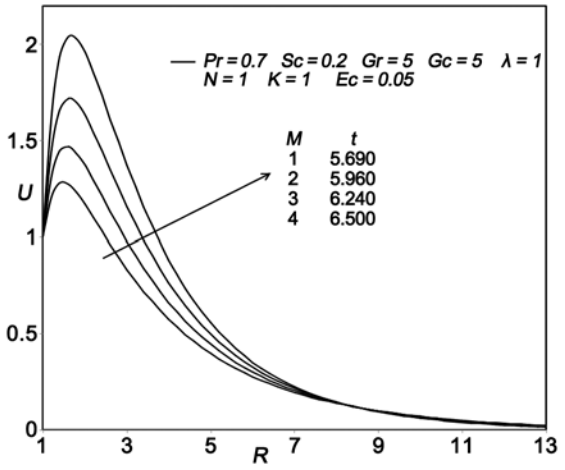

Fig. 5 — Velocity profile for Magnetic parameter *M*.

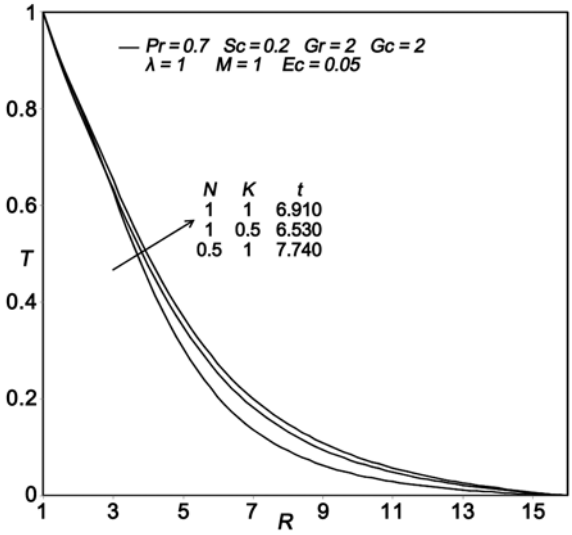

Fig. 6 — Temperature profiles for radiation parameter *N*.

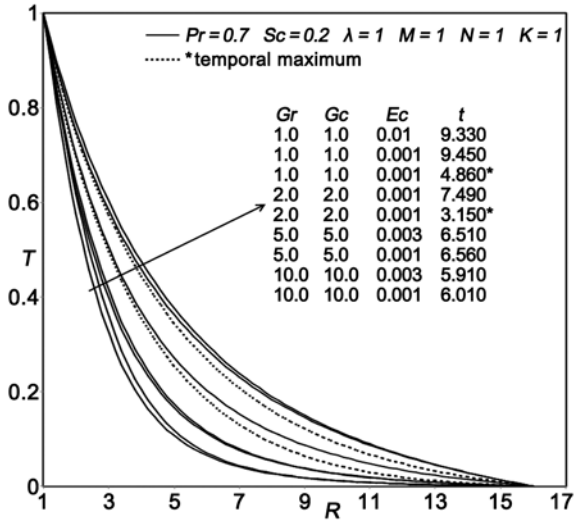

Fig. 7 — Temperature profiles for Steady state.

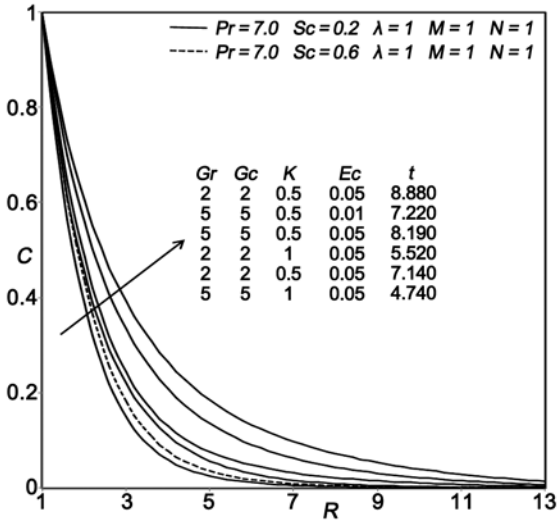

Fig. 8 — Concentration profile for Steady state.

Figure 6 provides the influence of radiation parameter N on the temperature at $X = 1.0$ for the case of air $Pr = 0.7$. It is inspected that an increase in the value of N leads to an increase in the value of temperature. This implies that the thermal radiation enhances the flow due to convection which in turn increases the thermal boundary layer. Time taken to reach steady state decreases with increasing value of radiation parameter N.

Figure 7 shows the steady state temperature profile for various values of Eckert number Ec and Grashof number for heat transfer Gr, when $Pr = 0.7$. It is observed that decreasing the value of Gr increases the temperature. Time taken to reach steady state decreases with increasing value of Gr. It is also perceived that the temperature increases as Ec increases. If the influence of viscous dissipation heat is predominant then there will be a rise in temperature. Also, time taken to reach steady state decreases with increasing value of Eckert number. The temporal maximum curves of the temperature are also shown in this graph.

Figure 8 illustrates the influence of Eckert number, Schmidt number, chemical reaction parameter and Grashof number for mass transfer on concentration profile for the case of air $Pr = 0.7$. Increasing the value of Ec leads to a decrease in the concentration. It is also observed that the time taken to reach steady state decreases with decreasing value of Eckert number. It is inspected that decreasing the value of Gc leads to an increase in the concentration.

Increasing the value of Schmidt number decreases the concentration, due to the influence of mass diffusivity of the fluid. Similarly, increasing the value of K decreases the value of concentration. This implies that increase in the Schmidt number and chemical reaction parameter leads to a decrease in the concentration boundary layer thickness. Also, the time taken reach steady state decreases with increasing values of Schmidt number and chemical reaction parameter.

The values of velocity, temperature and concentration are known numerically, so now we are interested in calculating the local and mean values of skin-friction coefficient, Nusselt number and Sherwood number. These are given as follows:

$$\tau_x = -\left(\frac{\partial U}{\partial R}\right)_{R=1} \quad \ldots (19)$$

$$\bar{\tau} = -\int_0^1 \left(\frac{\partial U}{\partial R}\right)_{R=1} dX \quad \ldots (20)$$

$$Nu_X = -X\left(\frac{\partial T}{\partial R}\right)_{R=1} \quad \ldots (21)$$

$$\overline{Nu} = -\int_0^1 \left(\frac{\partial T}{\partial R}\right)_{R=1} dX \quad \ldots (22)$$

$$Sh_X = -X\left(\frac{\partial C}{\partial R}\right)_{R=1} \quad \ldots (23)$$

$$\overline{Sh} = -\int_0^1 \left(\frac{\partial C}{\partial R}\right)_{R=1} dX \quad \ldots (24)$$

Five-point approximation formula is used to evaluate the derivatives involved in Eqs (19-24) and Newton Cotes formula is applied to evaluate the integrals involved in Eqs (19-24).

Figure 9 shows the behaviour of local wall shear stress for various values of Pr, λ, M and Ec. For highly viscous fluids the effect of wall shear stress is highly significant. That is, increasing the value of Pr leads to an increase in local wall shear stress. Also, it is perceived that decreasing the values of λ, M and Ec increases the value of local skin friction coefficient.

Figure 10 illustrates the influence of Prandtl number, Eckert number and Grashof number for heat transfer Gr on local Nusselt number for increasing values of X. It is observed that increasing the value of Pr and Gr, leads to an increase in the value of local Nusselt number. It is also examined that decreasing the value of Ec increases the local rate of heat transfer.

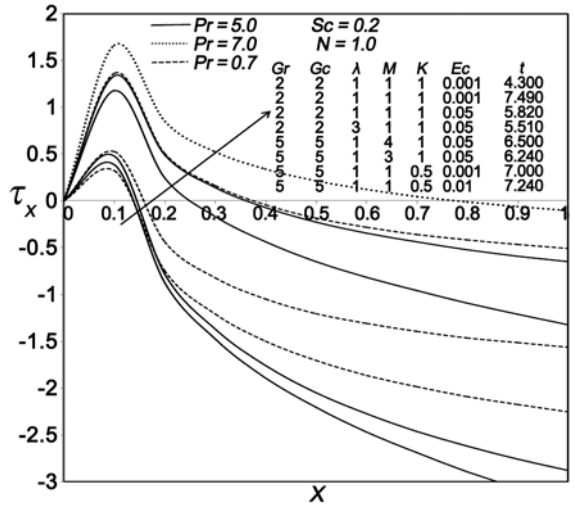

Fig. 9 — Local skin friction coefficient.

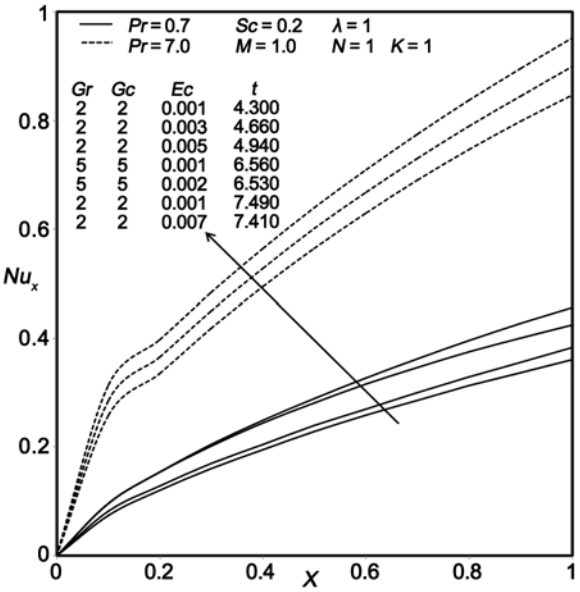

Fig. 10 — Local Nusselt number.

Figure 11 depicts the behaviour of local Sherwood number for different values of Schmidt number, Eckert number and chemical reaction parameter. It is inspected that increasing the value of Sc leads to an increase in the local mass transfer rate.

Figure 12 depicts the mean wall shear stress for different values of Pr and is plotted as a function of time. It is examined that increasing the value of Prandtl number increases the value of average skin friction coefficient. Increasing the value of magnetic parameter leads to an increase in the wall shear stress. This implies that drag force is influenced by the Lorentz force. It is also observed that decreasing the values of λ and Ec increases the skin friction.

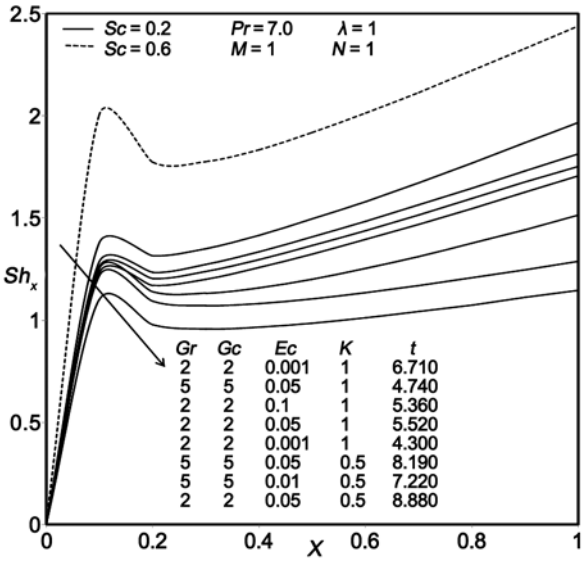

Fig. 11 — Local Sherwood number.

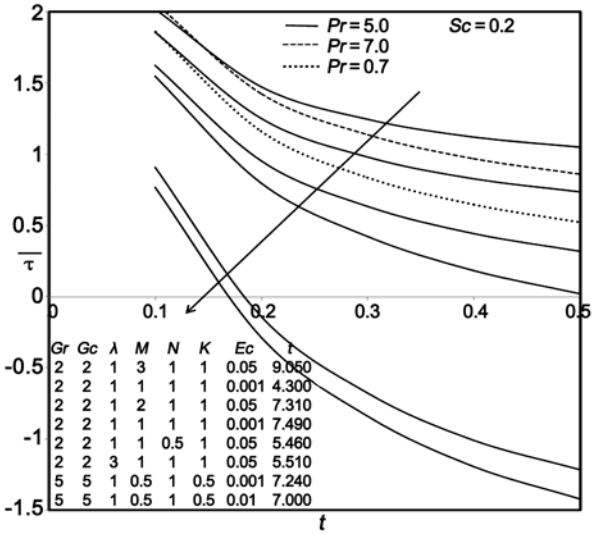

Fig. 12 — Mean skin friction coefficient.

Figure 13 illustrates the influence of Prandtl number and Eckert number on the rate of heat transfer and it is plotted as a function of time. It is noted the heat transfer rate increases with increasing value of Prandtl number *Pr.* This shows that for large values of *Pr*, thickness of the thermal boundary layer becomes small. It is also perceived that the rate of heat transfer increases with decreasing value of Eckert number *Ec.*

Figure 14 shows the mean Sherwood number for two different values of *Sc* against time *t*. It is examined that increasing the value of Schmidt number *Sc* leads to an increase in the rate of mass transfer. It is also observed that increasing the value of chemical reaction parameter increases the mean

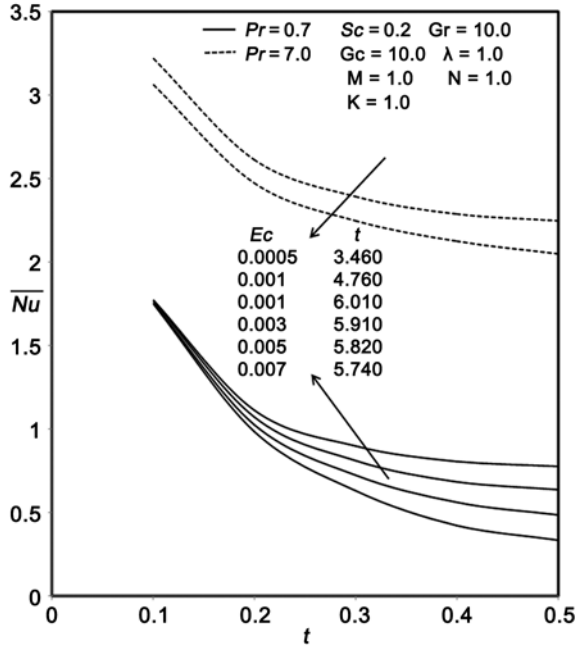

Fig. 13 — Mean Nusselt number.

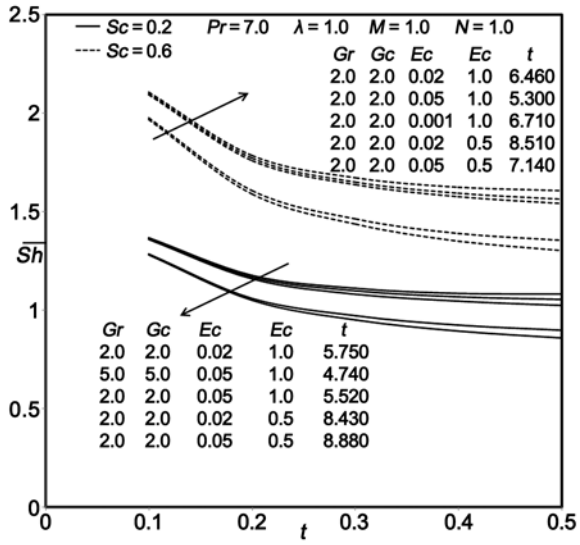

Fig. 14 — Mean Sherwood number.

Sherwood number. It can be seen that the rate of mass transfer is highly influenced by the chemical reaction parameter *K*. Increasing the value of *Gc* also increases the mass transfer rate due to buoyancy force. It is also inspected that the mass transfer rate gets increased for decreased values of Eckert number *Ec.*

6 Conclusions

In this paper, a numerical study has been performed for the transient free convective flow of a dissipative, chemically reacting fluid over a moving

semi-infinite vertical cylinder in the presence of porous medium. The influence of thermal radiation and transverse magnetic field are also under consideration. The non-dimensional form of momentum, energy and concentration equations are solved numerically using implicit finite difference scheme of Crank Nicholson type. The following results are obtained.

(i) The time taken to reach the steady state in velocity, temperature and concentration profiles is less, when Gr and Gc values are taken as large.

(ii) The velocity increases when the permeability of the material gets increased. The velocity gets increased for decreasing values of the magnetic parameter M. This is due to the influence of Lorentz force which reduces the tendency of the motion of fluid.

(iii) The influence of thermal radiation gives rise to an increase in temperature because it produces a significant change in the thermal condition of the fluid and its thermal boundary layer. The effect of viscous dissipation also increases the temperature. Since the conversion of kinetic energy in to internal energy by work done against the viscous fluid stresses causes a rise in the temperature as well as in the velocity.

(iv) The effects of chemical reaction parameter K leads to an increase in concentration. Increasing the value of Schmidt number decreases the concentration.

(v) Skin friction is more for higher values of Pr, since viscous effects are highly significant.

(vi) The rate of heat transfer increases with increasing values of Pr. It can be concluded that the velocity boundary layer develops faster than the thermal boundary layer for increasing values of Pr. So the velocity boundary layer thickness is predominant. It is perceived that decreasing the values of Eckert number enhances the heat transfer rate.

(vii) The rate of mass transfer increases with increasing values of Sc. Since the Schmidt number relates the viscous boundary layer and concentration boundary layer. Increase in Schmidt number leads to a decrease in the concentration boundary layer thickness. Also, the rate of mass transfer gets enhanced with increasing values of chemical reaction parameter K.

References

1 Minkowycz W J & Cheng P, *Int J Heat Mass Transfer*, 19 (1976) 805.
2 Yucel A, *Int J Heat Mass Transfer*, 33 (1990) 2265.
3 Gebhart B, *J Fluid Mech*, 14 (1962) 225.
4 Gebhart B & Mollendraf J, *J Fluid Mech*, 38 (1969) 97.
5 Basu T & Roy D N, *Int J Heat Mass Transfer*, 28 (1985) 699.
6 Nakayama A & Pop I, *Int Commun Heat Mass Transfer*, 16 (1989) 173.
7 Badruddin I A, Zainal Z A, Khan Z A & Mallick Z, *Int J Therm Sci*, 46 (2007) 221.
8 Muthucumaraswamy R, Kulandaivel T & Loganathan P, *Int J Math Anal*, 1 (2009) 1.
9 Poonia H & Chaudhary R C, *Theor Appl Mech*, 37 (2010) 263.
10 Rao J A & Shivaiah S, *Appl Math Mech Eng Ed*, 32 (2011) 1065.
11 Babu S M, Narayana S P V, Reddy S T & Reddy U D, *Adv Appl Sci Res*, 2 (2011) 226.
12 Singh J, *Ultra Sci*, 24 (2012) 335.
13 Khan M S, Karim I, Ali L E & Islam A, *Int Nano Lett*, 2 (2012) 1.
14 Mohammed Ibrahim S & Bhashar Reddy N, *ISRN Thermodyn*, (2013) 790604.
15 Reddy M G, *J Eng Phys Thermophys*, 87 (2014) 1233.
16 Haile E & Shankar B, *Am Chem Sci J*, 4 (2014) 828.
17 Narayana M, Khidir A A, Sibanda P & Murthy P V S N, *Trans Porous Med*, 96 (2013) 419.
18 Das K, *J Mech Sci Technol*, 28 (2014) 1881.
19 Ahmed S, Zueco J & Lopezochoa L M, *Chem Eng Commun*, 201 (2014) 419.
20 Raju M C, Ananda Reddy N & Varma S V K, *Ain Shams Eng J*, 5 (2014) 1361.
21 Reddy G J, Rao J A & Srinivasa R R, *Int J Adv Appl Math Mech*, 2 (2015) 164.
22 Balla C S & Naikoti K, *Alexandria Eng J*, 54 (2015) 661.
23 Sheri S R & Srinivasa Raju R, *Meccanica*, 51 (2015) 1057.
24 Pal D & Biswas S, *Int J Appl Comput Math*, 3 (2017) 1897.
25 Sreedevi G, Prasada Rao D R V, Makinde O D & Reddy V R G, *Indian J Pure Appl Phys*, 55 (2017) 551.
26 Reddy G J, Srinivasa Raju R & Rao J A, *Ain Shams Eng J*, (2017), in press.
27 Pandey A K & Kumar M, *Alexandria Eng J*, 56 (2017) 55.
28 Brewster M Q, *Thermal radiative transfer and properties*, (John Wiley & Sons New York), 1992, 378.
29 Carnahan B, Luther H A & Wilkes J O, *Applied Numerical methods*, (Wiley: New York), 1969, 441.
30 Chen T S & Yuh C F, *Int J Heat Mass Transfer*, 23 (1980) 451.